

Laser-Cluster-Interaction in a Nanoplasma-Model with Inclusion of Lowered Ionization Energies

P. Hilse, M. Moll, and M. Schlanges

Institut für Physik, Ernst-Moritz-Arndt-Universität, D-17487 Greifswald, Germany

Th. Bornath*

Institut für Physik, Universität Rostock, Universitätsplatz 3, D-18051 Rostock, Germany

(Dated: October 29, 2018)

The interaction of intense laser fields with silver and argon clusters is investigated theoretically using a modified nanoplasma model. Single pulse and double pulse excitations are considered. The influence of the dense cluster environment on the inner ionization processes is studied including the lowering of the ionization energies. There are considerable changes in the dynamics of the laser-cluster interaction. Especially, for silver clusters, the lowering of the ionization energies leads to increased yields of highly charged ions.

PACS numbers: 52.50.Jm, 52.25.Jm, 36.40.Gk, 52.38Dx

Keywords: laser matter interaction, cluster, nanoplasma, collisional absorption, ionization

I. INTRODUCTION

The interaction of intense laser radiation with clusters is a field of current interest. An important reason is that clusters present the advantage of high-energy absorption. Their interaction with electromagnetic fields is very effective because they are objects with initially solid-like atomic density in a nanometer scale size. Thus, absorption of energy is much larger in a cluster than for the corresponding atomic or bulk systems at the same intensities. Consequently, in laser-cluster experiments the emission of highly charged ions, very energetic electrons, higher order harmonics, fast fragments as well as strong x-rays in the multi-keV range is observed. Different theoretical models and simulations indicate that resonant collective absorption plays the central role. The rapid expansion of irradiated clusters is essential as, at a certain time, the cluster reaches the density fulfilling the resonance condition. This can occur during a single pulse. Another method which allows a better control is the dual-pulse laser excitation with varying time delay between two pulses [1]. Such experiments were performed recently for silver clusters showing a strong dependence of the highly charged ion yield as well as of the maximum energy of emitted electrons on the delay time [2].

For the theoretical description of such dynamical processes, there exist various methods. An overview about the different processes of laser-cluster interaction and about theoretical approaches is given, e.g., in [3, 4, 5]. More recently, a review on theoretical concepts to describe the energy absorption by clusters in the collisionless regime was given in [6]. One large group of methods are simulations ranging from classical molecular dynamics [7, 8, 9] used successfully for rare gas clusters, particle-in-cell methods [10, 11] to the so-called time-dependent local-density approximation coupled to ionic molecular dynamics [12] or the Thomas-Fermi-Vlasov molecular dynamics [13, 14] which treat the electrons in the cluster with density functionals and which have been especially applied for the description of metal clusters. In the latter method, the fermionic character of unbound electrons is resolved, the number of active electrons in this expensive calculations is, however, strongly limited.

Quite another method is the nanoplasma model introduced into cluster physics by Ditmire *et al.* [15]. In this model, the relevant processes are described by hydrodynamic balance equations and rate equations. For absorption and ionization rates, standard expressions are used. In order to understand the role of different absorption and ionization mechanisms in large clusters, this model seems to be suited because the influence of different approximations for the rates can be well controlled.

An interesting topic of current discussion is the influence of the dense cluster environment on the inner ionization processes itself. Here, screening and ionic microfield effects play an essential role. It has to be expected that the ionization energies of the various ions are lowered. There are different models whose applicability has to be investigated thoroughly [16, 17]. The entire process is not fully understood yet, however.

*Electronic address: thomas.bornath@uni-rostock.de

The aim of the present paper is to study the influence of correlation effects such as the lowering of the ionization energy on the dynamics of laser-cluster interaction determining current and internal electric field in a self consistent manner. In first calculations within the nanoplasma model [18, 19] we used an improved expression for collisional absorption which we derived recently for the bulk plasmas case [20, 21, 22, 23, 24] and considered the effect of the external field only to avoid unphysical enhancement of the internal field in a self consistent treatment. In the present paper, we follow [25, 26] to account for an additional damping term corresponding to electron-surface collisions. The central point is that we include the lowering of the ionization energies in the ionization rates. This lowering is calculated using the model of Stewart and Pyatt [27].

We give a brief description of the nanoplasma model and its modifications in Section 2. The consequences of lowered ionization energies on the dynamics of the interaction of silver and argon clusters with intense laser fields are discussed in Section 3 for the cases of single pulse excitation as well as for dual pulse excitation.

II. THE NANOPLASMA MODEL

The nanoplasma model allows to describe different physical processes like ionization, heating, and expansion that occur during the laser-matter interaction. In this section, a short review of the model is given and some generalizations are discussed. Especially, the influence of screening on the ionization rate will be considered. A further modification concerns the calculation of the heating due to collisional absorption.

The clusters are assumed to be initially neutral spheres with uniform temperature and density. It is assumed that there will be no gradients in density and temperature during the further evolution of the nanoplasma. The plasma will be heated due to the interaction with the laser radiation which is described by collisional absorption (inverse bremsstrahlung). The expansion and the resulting cooling of the plasma is modeled with hydrodynamic equations. For all processes, appropriate approximations have to be found to build up a system of rate equations for the plasma composition and a set of hydrodynamic equations in order to simulate the dynamics of the plasma.

A. Ionization

In the model, it is assumed that all electrons are bound before the cluster is irradiated with the laser beam. For tunnel ionization, cycle-averaged rates from Ammosov, Delone, and Krainov (ADK) [28] where used applied for the internal electric field of the cluster (see Section 2). The second important ionization process is electron impact ionization. Here one can distinguish ionization due to collisions with thermal electrons and ionization processes due to the directed oscillating motion of the electrons in the laser field [15]. The ionization rates for the various ionization stages are based on the semi-empirical cross sections of Lotz [29], for details, see also [19].

In a dense system, scattering processes are influenced by the surrounding medium. However, the evaluation of cross sections in strongly coupled systems is a demanding task. Undoubtly, the lowering of ionization energies is a main nonideality effect in dense Coulomb systems [30]. Here we use for the ionization rates due to impact of thermal electrons the simple relation [19, 31]

$$W_Z = W_Z^0 \exp\left(-\frac{\Delta_Z}{k_B T}\right) \quad (1)$$

with the ideal rates W_Z^0 calculated with the ionization cross sections for the isolated scattering event. Δ_Z is the shift of the ionization energy. According to (1) there is an exponential increase of the ionization rate with decreasing ionization energy.

For the lowering of ionization energy due to screening, Stewart and Pyatt [27] derived a formula interpolating between the cases of Debye screening and of the ion-sphere model. Consider the ionization reaction $A_{Z-1} \rightarrow A_Z + e^-$. In a plasma medium, the ionization energy $I_{Z-1} = I_{Z-1}^0 + \Delta_{Z-1}$ is lowered due to screening. Stewart and Pyatt have calculated the lowering of ionization potentials in plasmas beyond the Debye screening case. Starting from the finite-temperature Thomas-Fermi model, they evaluated the effect of the free electrons and the neighboring ions on the potential distribution around an ion. The following approximate formula could be derived:

$$\Delta_{Z-1} = -\frac{[3(Z^* + 1)\frac{Z\kappa e^2}{k_B T} + 1]^{2/3} - 1}{2(Z^* + 1)} k_B T \quad (2)$$

where κ is an effective inverse screening length

$$\kappa^2 = \frac{4\pi e^2}{k_B T} (Z^* + 1) n_e \quad (3)$$

with the free electron density n_e . Z^* is an effective charge number

$$Z^* = \frac{\langle Z^2 \rangle}{\langle Z \rangle} \quad \text{with} \quad \langle Z^k \rangle = \frac{\sum_{Z=0}^{Z_{\max}} n_Z Z^k}{\sum_{Z=0}^{Z_{\max}} n_Z} \quad (4)$$

where n_Z is the particle number density of ions with charge Z , Z_{\max} denotes the fully stripped ion.

Gets and Krainov have calculated recently [17] the ionization potentials for ions in rare gas clusters using the Schrödinger equation with the Debye potential. In a first-order perturbation approach using Coulomb matrix elements, they derived a shift which agrees well with numerical solutions of the Schrödinger equation. The Debye shift – which is the lowest order – overestimates the shift slightly. For stronger coupling, low temperature or high density, the calculated shift of Gets and Krainov is bigger than the Stewart-Pyatt shift. By using the Stewart-Pyatt model, it is possible to extend the description to parameter regions where the condition of linear screening is fulfilled no longer.

B. Plasma heating by collisional absorption

The balance equation for the electrical current density in a spherical cluster can be written in the following form

$$\frac{d}{dt} \mathbf{j}(t) - \frac{\omega_p^2}{4\pi} \mathbf{E}^{\text{ext}}(t) + \frac{\omega_p^2}{3} \int_{t_0}^t d\bar{t} \mathbf{j}(\bar{t}) = \sum_c \int \frac{d^3 p_c}{(2\pi\hbar)^3} \frac{e_c \mathbf{p}_c}{m_c} I_c(\mathbf{p}_c, t) \quad (5)$$

with the plasma frequency $\omega_p^2 = \sum_c \frac{4\pi e_c^2 n_c}{m_c}$ and I_c being the general collision integral for species c . The third term on the left hand side describes the polarization stemming from the mean field contribution. The right hand side of the above equation describes the friction $-\mathbf{R}$ due to collisions. The balance equation then can be written as

$$\begin{aligned} \frac{d}{dt} \mathbf{j}(t) + \mathbf{R}\{\mathbf{j}\} &= \frac{\omega_p^2}{4\pi} \mathbf{E}^{\text{ext}}(t) - \frac{\omega_p^2}{3} \int_{t_0}^t d\bar{t} \mathbf{j}(\bar{t}) \\ &= \frac{\omega_p^2}{4\pi} \mathbf{E}^{\text{int}}(t), \end{aligned} \quad (6)$$

where the internal electrical field was introduced in the second line. The friction term is a nonlinear non-Markovian functional of the current, $\mathbf{j} = \sum_c n_c e_c \mathbf{v}_c$, for details, see [19, 21, 24, 30]. Considering harmonic electrical fields, $\mathbf{E} = \mathbf{E}_0 \cos(\omega t + \phi)$, the component $R(\omega)$ can formally be written as $R(\omega) = \nu(\omega, j(\omega)) j(\omega)$, where the complex collision frequency, however, is dependent on the current. The balance equation takes the form

$$-i\omega j(\omega) + \nu(\omega) j(\omega) = \frac{\omega_p^2}{4\pi} E^{\text{int}}(\omega), \quad (7)$$

where $E^{\text{int}}(\omega)$ is the Fourier component of the internal field. We can introduce the field dependent (nonlinear) conductivity σ according to

$$j(\omega) = \sigma(\omega) E^{\text{int}}(\omega) = \frac{\frac{\omega_p^2}{4\pi}}{-i\omega + \nu(\omega)} E^{\text{int}}(\omega). \quad (8)$$

The quiver velocity v_{os} is given then by

$$v_{\text{os}} = \frac{|j(\omega)|}{e n_e} = \frac{e |E^{\text{int}}(\omega)|}{m_e |-i\omega + \nu(\omega)|}. \quad (9)$$

Approximately, one can use the familiar relation $v_{\text{os}} \approx e E^{\text{int}} / (m_e \omega)$.

External and effective field are connected by

$$\begin{aligned} E^{\text{int}}(\omega) &= \frac{\omega + i\nu(\omega)}{\left(\omega - \frac{\omega_p^2}{3\omega}\right) + i\nu(\omega)} E^{\text{ext}}(\omega) \\ &= \frac{3}{2 + \varepsilon(\omega)} E^{\text{ext}}(\omega), \end{aligned} \quad (10)$$

where we introduced the (macroscopic) dielectric function $\varepsilon(\omega)$ of the system which is connected to the internal conductivity by $\varepsilon(\omega) = 1 + \frac{i4\pi\sigma(\omega)}{\omega}$.

The energy absorption rate is given by

$$\frac{\langle \mathbf{j} \cdot \mathbf{E}^{\text{ext}} \rangle}{\frac{1}{4\pi} \langle \mathbf{E}^{\text{ext}} \cdot \mathbf{E}^{\text{ext}} \rangle} = \frac{\omega_p^2}{\left[\omega - \frac{\omega_p^2}{3\omega} - \text{Im}\nu(\omega) \right]^2 + [\text{Re}\nu(\omega)]^2} \text{Re}\nu(\omega).$$

Here the brackets denote cycle-averaged quantities [20, 32]. In particular, we have $\langle \mathbf{E}^{\text{ext}} \cdot \mathbf{E}^{\text{ext}} \rangle = |E_0|^2/2$ with E_0 being the amplitude of the external field. Often the imaginary part can be neglected, and we get for $dU/dt = \langle \mathbf{j} \cdot \mathbf{E}^{\text{ext}} \rangle$

$$\frac{dU}{dt} \approx \frac{\omega_p^2 \text{Re}\nu(\omega)}{8\pi} \frac{1}{\left[\omega - \frac{\omega_p^2}{3\omega} \right]^2 + [\text{Re}\nu(\omega)]^2} |E_0|^2, \quad (11)$$

which is, setting $\text{Re}\nu(\omega) = \nu$ (as usual), the same expression for the heating rate as in [15].

The dynamical collision frequency is dependent on the frequency of the field and, in general, also on the field strength. That's why the inner electrical field and the collision frequency have to be determined in a self consistent manner, see eqs. (9) and (10). Taking into account only electron-ion collisions, cf. eq. (13), the inner electrical field is enhanced in the vicinity of the Mie resonance condition, $\omega \approx \omega_p/\sqrt{3}$, unphysically strong. There are different attempts to avoid this behavior, e.g., [25, 33]. Popruzhenko et al. [6] have given a thorough discussion of such mechanisms in terms of collisionless absorption. Here we follow [25, 26], and consider not only collisions of electrons with individual ions but also with the surface of the cluster. Therefore, we will use

$$\nu(\omega) = \text{Re}\nu_{ei}(\omega) + \nu_s(\omega), \quad (12)$$

For the electron-ion collision frequency ν_{ei} , an expression is used which has been derived in a quantum statistical approach for the case of bulk plasmas [21, 24, 30].

$$\text{Re}\nu_{ei} = \frac{16\pi n_i Z^2 e^4}{\omega_p^2 m_e^2 v_{os}^2} \int \frac{d^3q}{(2\pi\hbar)^3} \sum_{m=1}^{\infty} m\omega J_m^2 \left(\frac{\mathbf{q} \cdot \mathbf{v}_{os}}{\hbar\omega} \right) V(q) \mathcal{S}_{ii}(\mathbf{q}) \text{Im}\varepsilon^{-1}(\mathbf{q}, -m\omega) \quad (13)$$

where n_i and e_i denote the ion density and charge, J_m are Bessel functions of the first kind, $V(q) = 4\pi\hbar^2/q^2$, \mathcal{S}_{ii} denotes the static ion-ion structure factor, and ε is the Lindhard dielectric function for the electrons. This expression does not involve a Coulomb logarithm. The quantum statistical treatment [20, 34] automatically leads to convergent expressions for the collision frequency for higher coupling where the classical results break down because some cut-off is introduced [35] leading to the Coulomb logarithm. Strong correlations of the ionic subsystem are expressed by the ionic structure factor. Cold ions decrease the collision frequency in a wide range of the plasma-parameters [22, 23] what was also confirmed by molecular dynamics simulations [22].

The electron-surface collision frequency is taken as [25, 26]

$$\nu_s = \frac{\sqrt{v_{th}^2 + v_{os}^2}}{r} \quad (14)$$

with the cluster radius r , the thermal velocity v_{th} and the quiver velocity v_{os} .

C. Cluster expansion

After formation of the nanoplasma, the clusters are expanding during and after the laser pulse mainly due to the pressure of the hot electrons and a possible charge buildup at the cluster. Heating of the plasma via inverse bremsstrahlung as well as the production of electrons in ionization processes lead to an increasing electron pressure with the consequence that the plasma will expand in the surrounding vacuum. This expansion is governed by the following equation [4] (please note, that there is a misprint in eq. (27) in [15])

$$\frac{d^2r}{dt^2} = 5 \frac{p_e + p_{\text{coul}}}{n_i m_i} \frac{1}{r} \quad (15)$$

where r denotes the plasma radius, and n_i, m_i are the ion density and mass. The pressure is taken here as the ideal electron Fermi gas pressure. The Coulomb pressure contribution p_{coul} due to a charge buildup [15] is comparatively small in the calculations following below.

The expansion of the cluster leads to a cooling. The equation of motion for the temperature is

$$\frac{dT}{dt} = -2\frac{T}{r}\frac{dr}{dt} + \frac{1}{c}\frac{dU}{dt}. \quad (16)$$

Here $\frac{dU}{dt}$ is the expression (11) for the energy impact and $c = 3/2n_e k_B$ is the heat capacity of an ideal gas.

III. NUMERICAL RESULTS

First, we adopt single laser pulses with a Gaussian shape in the intensity profile and a full width at half of the maximum (FWHM) of 130fs. The wavelength of the laser is chosen to be 825nm. The Mie resonance can occur therefore at an electron density $n_e = 3n_{\text{crit}}$ with a critical plasma density $n_{\text{crit}} = 1.64 \times 10^{21}\text{cm}^{-3}$. Most of the calculations are for silver clusters. Furthermore, argon clusters are considered.

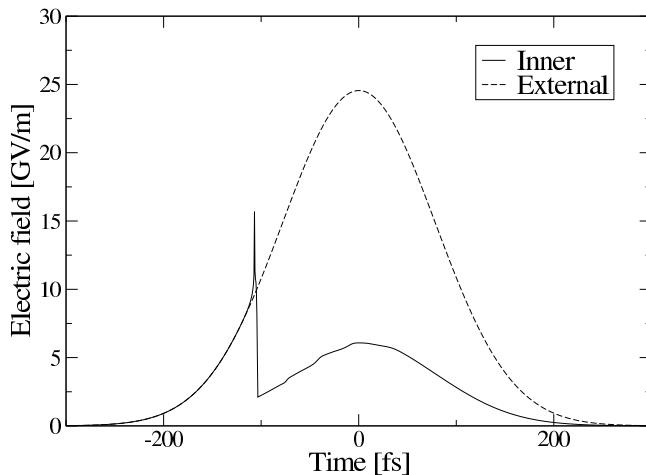


FIG. 1: External and inner electrical fields in a silver nanoplasma with initial cluster diameter of 60nm. The 130 fs laser pulse at 825 nm has a peak intensity of 80 TWcm^{-2} .

As already mentioned above, the nanoplasma model represents a coupled set of hydrodynamic and rate equations, which allows a description of the dynamics of the interaction of intense laser fields with clusters. In particular, the temporal evolution of, e.g., the density, the cluster radius, the electron temperature, and the occupation numbers of the different ionic charge states can be calculated. In the present calculations, special attention is paid to the influence of the lowering of the ionization energy on dynamics of the laser-cluster interaction. Concerning the heating and ionization rates, eq. (6) cannot be solved simply for j in the general case. Current and internal field have to be determined in a self consistent manner according to eq. (9) and eq. (10) with a collision frequency ν depending on the internal field via the quiver velocity v_{os} in a nonlinear way.

Results for the internal field in a silver cluster with an initial diameter of 60 nm irradiated by 130 fs laser pulse with a peak intensity of 80 TWcm^{-2} are shown in Fig. 1. Free charges are produced in the beginning of the laser-cluster interaction by tunnel ionization. The produced nanoplasma is then heated by collisional absorption, and a further increase of the densities of free charges is mainly determined by the electron impact ionization processes. The internal field increases up to the Mie resonance which is reached for an electron density $n_e = 3n_{\text{crit}}$. There, an enhanced peak occurs followed by a sharp decrease of the internal field. After the resonance the electron density remains overcritical up to the end of the laser pulse (see also Fig. 3) leading to values of the internal field considerably lower than those of the external one.

Electron temperature and density in a silver cluster with an initial diameter of 60 nm are shown in Figs. 2 and 3 as a function of time. Three different peak intensities of 80 TWcm^{-2} , 500 TWcm^{-2} , and 3 PWcm^{-2} are considered. Temperature and density rise quickly at the beginning of the interaction of the laser pulse with the cluster. The step-like behavior of the electron density reflects the inner sequential ionization of the ions in different charge states. For a pulse with higher intensity, temperature and density are higher, as expected. For long times, there is a stronger decrease of density and temperature for pulses with higher intensities which is a consequence of faster expansion.

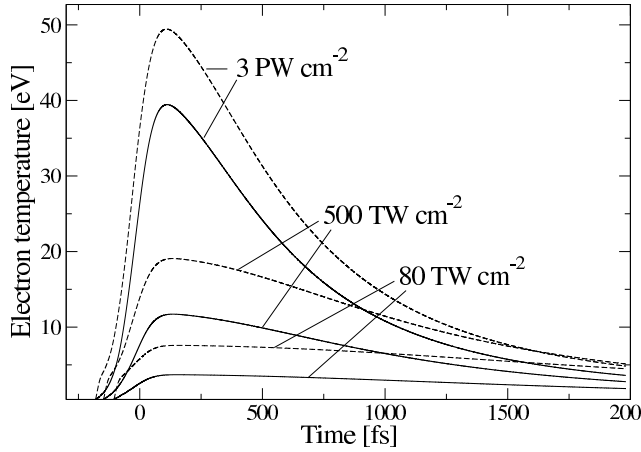


FIG. 2: Electron temperature as a function of time for a silver nanoplasma with initial cluster diameter of 60nm for different intensities of the 130 fs pulse at 825 nm. Solid line: Lowering of ionization energies with Stewart-Pyatt shift. Dashed line: No shift.

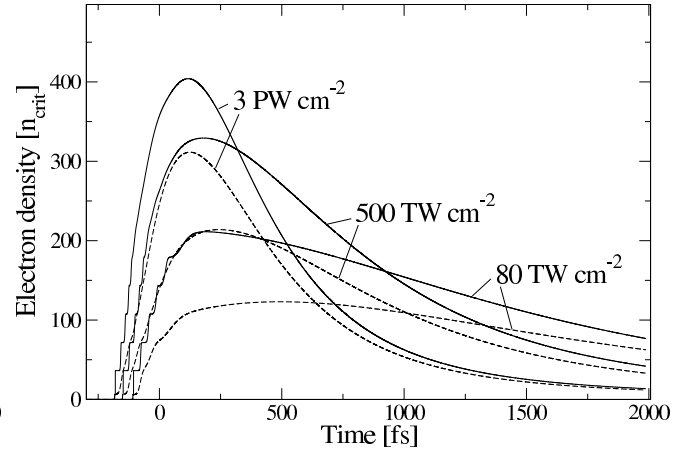


FIG. 3: Electron density as a function of time for a silver nanoplasma with initial cluster diameter of 60nm for different intensities. The pulse parameters are the same as in Fig. 2. Solid line: Lowering of ionization energies with Stewart-Pyatt shift. Dashed line: No shift.

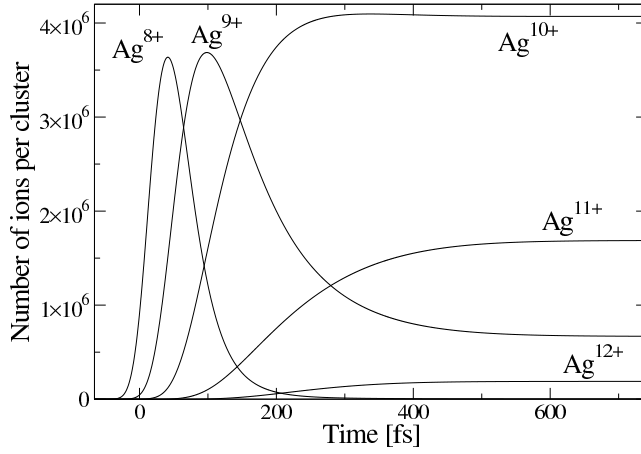


FIG. 4: Composition as a function of time for a silver nanoplasma with initial cluster diameter of 60nm. There was no shift of ionization energies considered in this calculation. The laser pulse is Gaussian with 130fs length and a peak intensity of 3PWcm^{-2} .

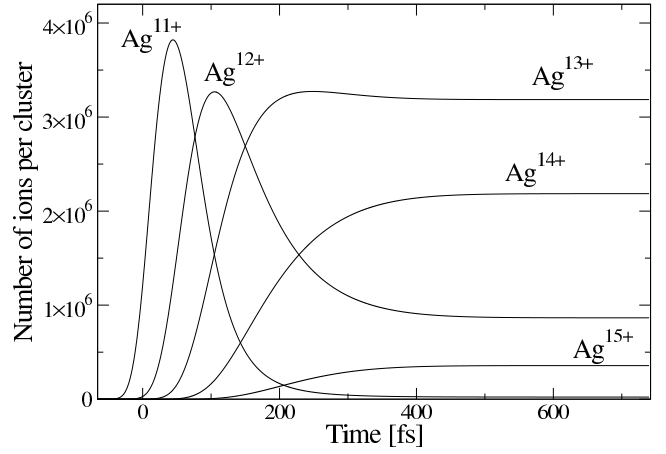


FIG. 5: Composition as a function of time for a silver nanoplasma with initial cluster diameter of 60nm. Lowering of ionization energies with Stewart-Pyatt shift is included. The pulse parameters are the same as in Fig. 4.

An important result are the consequences of the lowering of the ionization energies which we included in our model using generalized (nonideal) impact ionization rates. The inclusion of this nonideality effect (solid lines) leads to lower electron temperatures whereas the electron densities are higher compared to the results using the usual ideal rates (dashed lines). Due to the lowering of the ionization energies, the number of ionization events in the dense nonideal nanoplasma is higher.

The consequences on the population dynamics for the different ionic charge states are shown in Figs. 4 and 5. A silver cluster is considered with an initial diameter of 60 nm irradiated by a pulse with a peak intensity of 3PWcm^{-2} . The comparison shows that the inclusion of the lowering of the ionization energies in the model leads to the population of considerable higher ionic charge states compared to the results using the usual ideal ionization rates. As can be

seen from Fig. 5, mainly Ag^{11+} and Ag^{12+} are populated during the laser pulse with 130 fs (FWHM). For later times, i.e. in the expansion phase after the pulse, Ag^{13+} and Ag^{14+} are the dominating ionic charge states whereas Ag^{10+} and Ag^{11+} are the dominating species using the usual ideal rates (see Fig. 4).

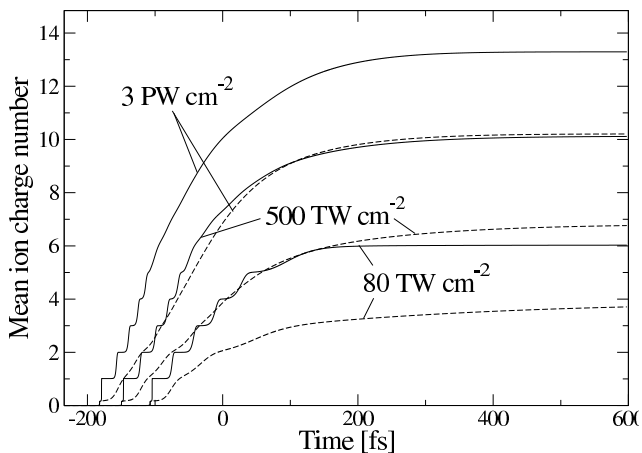


FIG. 6: Mean charge number as a function of time for a silver nanoplasma with initial cluster diameter of 60 nm for different intensities of single 130 fs pulses at 825 nm. Solid line: Lowering of ionization energies with Stewart-Pyatt shift. Dashed line: No shift.

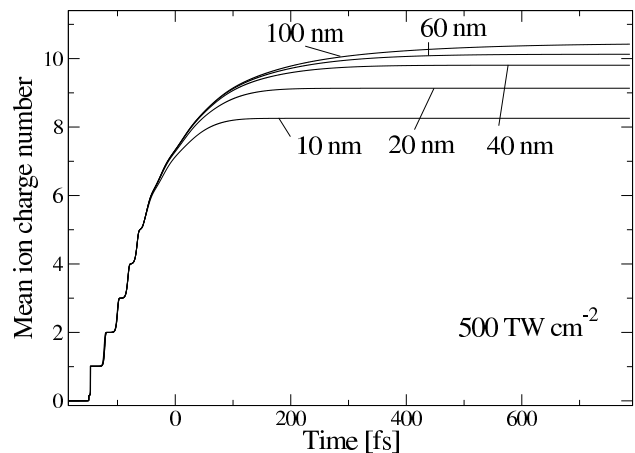


FIG. 7: Mean charge number as a function of time for silver clusters with different initial cluster diameters for 500 TW cm^{-2} peak intensity of single 130 fs pulses at 825 nm.

The mean ionic charge number vs. time is shown in Fig. 6 for a silver cluster with an initial diameter of 60 nm. Again the two variants of the calculation (with and without lowered ionization energies) are compared for the three different peak intensities of 80 TW cm^{-2} , 500 TW cm^{-2} , and 3 PW cm^{-2} . As in Fig. 3, the step-like behavior at the beginning of the laser-cluster interaction reflects the ionization of the ionic species in the different charge states. The higher the intensity the earlier the mean ion charge number begins to increase up to a constant value for longer times after the pulse. For the higher intensities, the mean charge state is increased by a value of about three compared to that following from the calculations using ideal rates (dashed).

An interesting question is how the mean ionic charge number calculated within our model depends on the cluster size. Results concerning this question are presented in Fig. 7. In particular, the mean charge is shown as a function of time for clusters with different initial diameters irradiated by a laser pulse with peak intensity of 500 TW cm^{-2} . In the early stage of the laser-cluster interaction a step-like increase of the mean charge number is observed without remarkable differences between the results for the different cluster sizes. Essential deviations appear after the maximum of the pulse: with increasing cluster size, the mean ionic charge number increases, i.e. for larger clusters the impact ionization is more efficient during the cluster expansion compared to smaller clusters.

Let us now investigate the ionization dynamics in a rare gas cluster. As an example, we consider an argon cluster with an initial diameter of 60 nm irradiated by a laser pulse with 130 fs length (FWHM) and peak intensity of 10 PW cm^{-2} . Again, we compare the results for the population dynamics of the different ionic charge states following from calculations without and with inclusion of the lowering of the ionization energies. There are not such drastic changes concerning the dominating charge states as compared to silver clusters what results from the differences in the energy spectra. For long times, there are relatively small quantitative differences for the population of the dominating charge state Ar^{13+} .

Finally, we present results for double pulse excitation of silver clusters as investigated recently in experiments by Döppner et al. [2]. In our calculations, the laser radiation was simulated by two pulses with Gaussian shape in the intensity profile with a duration of 130 fs (FWHM) and a peak intensity of 80 TW cm^{-2} for each pulse. The wavelength was 825 nm. Numerical results for the yield of Ag^{10+} ions as a function of the delay time for a silver cluster with an initial diameter of 10 nm are shown in Fig. 10. We observe a well-developed increase of the yield of Ag^{10+} near a certain optimum delay time with a maximum at a delay of 1467 fs. To explain this, one has to examine the dynamics of the dense nanoplasma during the laser irradiation more in detail. The first pulse reaches its maximum at $t=0$ fs. It creates, via tunnel ionization and, later, thermal ionization, a large overcritical electron density. After the first pulse, the cluster expands and the electron density decreases. The heating of the second pulse

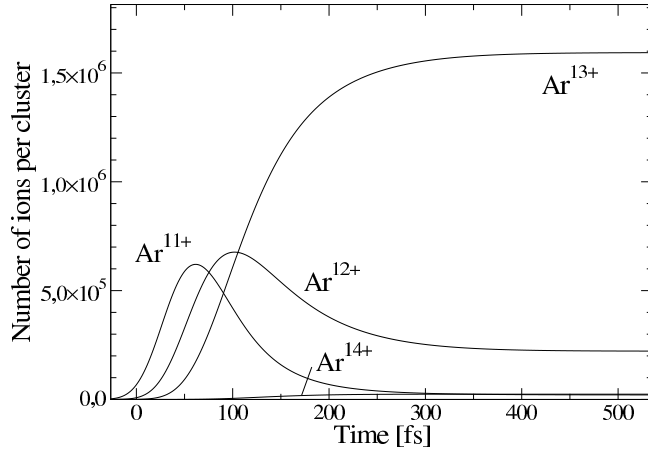


FIG. 8: Composition as a function of time for an argon nanoplasma with initial cluster diameter of 60nm. There was no shift of ionization energies considered in this calculation. The laser pulse is Gaussian with 130fs length and a peak intensity of 10PWcm^{-2} .

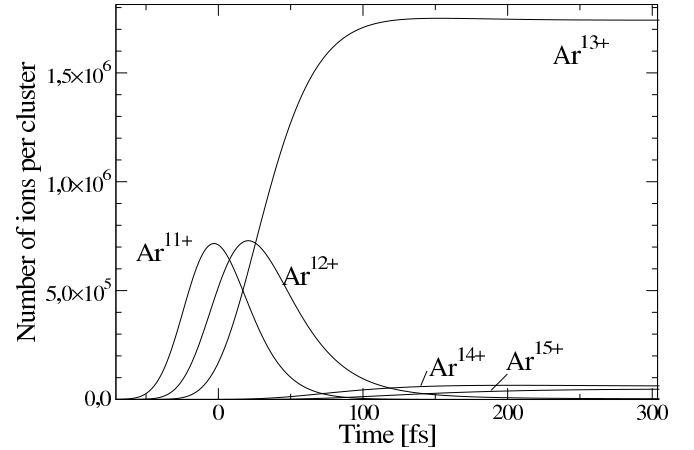


FIG. 9: Composition as a function of time for an argon nanoplasma with initial cluster diameter of 60nm. Lowering of ionization potentials with Stewart-Pyatt shift is included. The pulse parameters are the same as in Fig. 8.

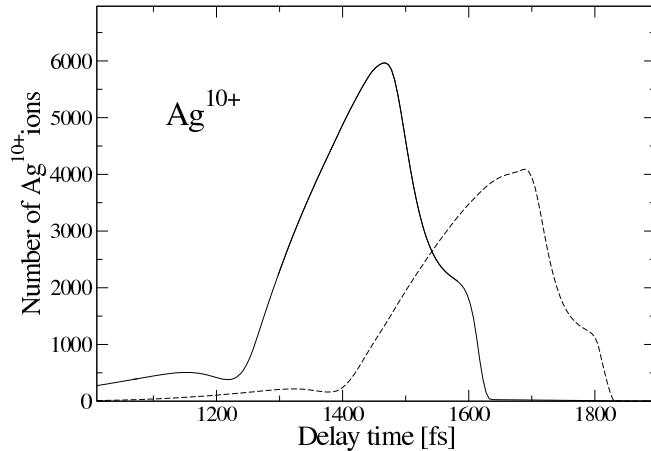


FIG. 10: Yield of Ag^{10+} for silver clusters with an initial diameter of 10 nm irradiated by a double pulse as a function of the delay time. The pulses have a peak intensity of 80TWcm^{-2} and a duration of 130 fs (FWHM). The wavelength is 825 nm. Solid line: Lowering of the ionization energies with the Stewart-Pyatt shift. Dashed line: no shift.

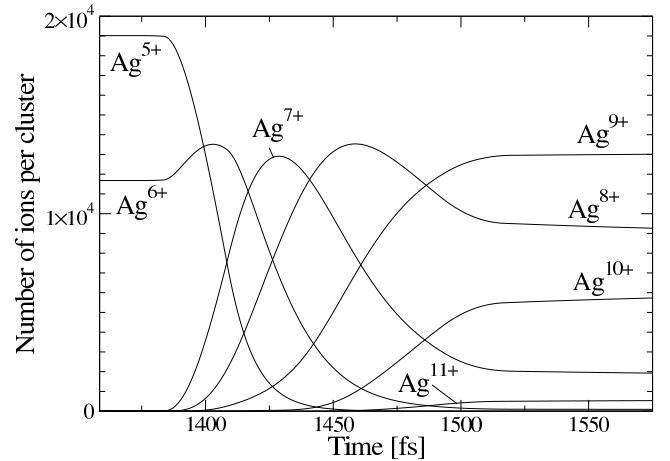


FIG. 11: Composition in a silver nanoplasma as a function of time for a double pulse with a delay time of 1467 fs. The initial cluster diameter is 10 nm, and the pulse parameters are the same as in Fig. 10 (with shift).

depends strongly on the applied delay time. Choosing the delay of the second pulse in such a way that it hits the cluster at about $3n_{\text{crit}}$ one excites the cluster resonantly which leads to the Ag^{10+} yield shown in Fig. 10. This is in qualitative agreement with the experimental results where, however, the optimum delay time was found to be of about 3 times larger. To explain this deviation, a more detailed analysis of the experimental conditions is necessary. For instance, a cluster size distribution was used in the considered experiment in contrast to the calculations where a single cluster size was assumed. In our calculations the maximum Ag^{10+} ion yield is higher, and it is shifted to a shorter optimum delay if the lowering of the ionization energy is included (solid line). A more complicated structure

of the Ag^{10+} ion yield as a function of the delay time is found for larger clusters which will be discussed elsewhere.

Fig. 11 shows the calculated population of the different ionic charge states as a function of time with a delay of 1467 fs for the considered cluster. The first pulse creates silver ions with Ag^{5+} and Ag^{6+} being the dominant species. The second pulse with the same intensity and duration creates considerable higher ionic charge states with Ag^{10+} being one of the dominant species.

IV. CONCLUSION

We investigated theoretically the ionization dynamics in silver clusters and also in argon clusters irradiated by intense laser pulses within the nanoplasma model. Single pulse and double pulse excitations were considered applying pulses with a Gaussian shape in the intensity profile. The calculations were performed for pulses with the same length of 130 fs (FWHM), but for different peak intensities. Clusters with initial diameters between 10 nm and 100 nm were considered. The dynamics of the laser-cluster interaction for single pulse excitation was studied more in detail for clusters with an initial diameter of 60 nm.

Special attention was paid to the consequences of the inclusion of the lowering of the ionization energies on the dynamics of the laser-cluster interaction within the nanoplasma model. In the regime of the dense nonideal nanoplasma, the bound state properties can be strongly affected by the interaction with the surrounding particles. An important effect is the ionization energy suppression which was treated in the present paper in the Stewart-Pyatt approach. The change of the reaction rates due to the lowering of the ionization energies was taken into account by a simple analytical formula which allows a qualitative correct description.

The comparison of calculations with the usual ideal rates with the nonideal rates shows significant changes in the ionization dynamics for silver clusters. Considerable higher ionic charge states occur to be the dominant species if nonideal rates are used in the model. Smaller changes are observed for argon clusters due to the differences in the energy spectra.

Motivated by recent experiments, the dynamics of laser-cluster interaction for double pulse excitation of silver clusters was studied within the present model at the end of the paper. A well-developed increase of the yield of Ag^{10+} ions near a certain optimum delay time between the two pulses was obtained which is in qualitative agreement with the experimental results. At the optimum delay the second pulse excites the cluster resonantly at about $3n_{\text{crit}}$ which leads to an increased yield of highly charged ions.

Acknowledgments

This work was supported by the Deutsche Forschungsgemeinschaft (SFB 652). We acknowledge valuable discussions with T. Döppner, T. Fennel, K.-H. Meiwes-Broer, and J. Tiggesbäumker.

-
- [1] T. Döppner, Th. Fennel, Th. Diederich, J. Tiggesbäumker, and K.-H. Meiwes-Broer, *Phys. Rev. Lett.* **94**, 013401 (2005).
 - [2] T. Döppner, Th. Fennel, P. Radcliffe, J. Tiggesbäumker, and K.-H. Meiwes-Broer, *Phys. Rev. A* **73**, 031202(R) (2006).
 - [3] V.P. Krainov and M.B. Smirnov, *Physics Reports* **370**, 237 (2002).
 - [4] P.-G. Reinhard and E. Suraud, *Introduction to Cluster Dynamics* (Wiley, Weinheim, 2004).
 - [5] U. Saalman, Ch. Siedschlag, and J.M. Rost, *J. Phys. B: At. Mol. Opt. Phys.* **39**, R39 (2006).
 - [6] S.V. Popruzhenko, D.F. Zaretsky, and D. Bauer, *Laser Phys. Lett.* **5**, 631 (2008).
 - [7] U. Saalman and J.-M. Rost, *Phys. Rev. Lett.* **91**, 223401 (2003).
 - [8] S. V. Fomichev, D. F. Zaretsky, D. Bauer, and W. Becker, *Phys. Rev. A* **71**, 013201 (2005).
 - [9] Th. Fennel, L. Ramunno, and Th. Brabec, *Phys. Rev. Lett.* **99** 233401 (2007).
 - [10] C. Jungreuthmayer, M. Geissler, J. Zanghellini, and Thomas Brabec, *Phys. Rev. Lett.* **92**, 133401 (2004).
 - [11] M. Kundu and D. Bauer, *Phys. Plasmas* **15**, 033303 (2008).
 - [12] P.-G. Reinhard and E. Suraud, *Appl. Phys. B* **73**, 401 (2001).
 - [13] Th. Fennel, G. F. Bertsch, and K.-H. Meiwes-Broer, *Eur. Phys. J. D* **29**, 367 (2004).
 - [14] Th. Fennel, T. Döppner, J. Passig, Ch. Schaal, J. Tiggesbäumker, and K.-H. Meiwes-Broer, *Phys. Rev. Lett.* **98**, 143401 (2007).
 - [15] T. Ditmire, T. Donnelly, A. M. Rubenchik, R. W. Falcone, and M. D. Perry, *Phys. Rev. A* **53**, 3379 (1996).
 - [16] S. Micheau, F.A. Gutierrez, B. Pons, and H. Jouin, *J. Phys. B: At. Mol. Opt. Phys.* **38** 3405 (2005).
 - [17] A.V. Gets and V. P. Krainov, *J. Phys. B: At. Mol. Opt. Phys.* **39**, 1787 (2006).
 - [18] Th. Bornath, P. Hilse, and M. Schlanges, *Contrib. Plasma Phys.* **47** 402 (2007).
 - [19] Th. Bornath, P. Hilse, and M. Schlanges, *Laser Physics* **17** 591 (2007).

- [20] Th. Bornath, M. Schlanges, P. Hilse, and D. Kremp, Phys. Rev. E **64**, 026414 (2001).
- [21] Th. Bornath, M. Schlanges, P. Hilse, and D. Kremp, J. Phys. A: Math. Gen. **36**, 5941 (2003).
- [22] P. Hilse, M. Schlanges, Th. Bornath, and D. Kremp, Phys. Rev. E **71**, 056408 (2005).
- [23] D. Semkat, R. Redmer, and Th. Bornath, Phys. Rev. E **73**, 066406 (2006).
- [24] Th. Bornath and M. Schlanges, J. Phys. A: Math. Gen. **39**, 4699 (2006).
- [25] F. Megi, M. Belkacem, M.A. Bouchene, E. Suraud, and G. Zwicknagel, J. Phys. B: At. Mol. Opt. Phys. **36**, 273 (2003).
- [26] S. Micheau, H. Jouin, and B. Pons, Phys. Rev. A **77**, 053201 (2008).
- [27] J.P. Stewart and K.D. Pyatt, ApJ **144**, 1203 (1966).
- [28] M. V. Ammosov, N. B. Delone, and V.P. Krainov, Zh. Eksp. Teor. Fiz. **19**, 2008 (1968) [Sov. Phys. JEPT **64**, 1191 (1986)].
- [29] W. Lotz, Z. Phys. **216**, 241 (1968).
- [30] D. Kremp, M. Schlanges, and W.-D. Kraeft, *Quantum Statistics of Nonideal Plasmas* (Springer, Berlin Heidelberg, 2005).
- [31] M. Schlanges, Th. Bornath, and D. Kremp, Phys. Rev. A **38**, 2174 (1988).
- [32] Th. Bornath, M. Schlanges, P. Hilse, and D. Kremp in: *Nonequilibrium Physics at Short Time Scales*, ed. by K. Morawetz (Springer, Berlin, 2004) 154.
- [33] J. Liu, R. Li, P. Zhu, Z. Xu, and J. Liu, Phys. Rev. A **64**, 033426 (2001).
- [34] H.-K. Kull and L. Plagne, Phys. Plasmas **8**, 5244 (2001).
- [35] C.D. Decker, W.B. Mori, J.M. Dawson, and T. Katsouleas, Phys. Plasmas **1**, 4043 (1994).